Multidisciplinary ⋮ Rapid Review ⋮ Open Access Journal

Date of publication xxxx 00, 0000, date of current version xxxx 00, 0000.

Digital Object Identifier 10.1109/ACCESS.2017.Doi Number

Varietal Classification of Rice Seeds using RGB and Hyperspectral Images

Samson Damilola Fabiyi[1], Hai Vu[2], Christos Tachtatzis[1], Paul Murray[1], David Harle[1], Trung Kien Dao[2], Ivan Andonovic[1], Jinchang Ren[1], Stephen Marshall[1]

[1]Department of Electronic and Electrical Engineering, University of Strathclyde, Glasgow, United Kingdom

[2]International Research Institute MICA, Hanoi University of Science and Technology, Hanoi, Vietnam

Corresponding author: Samson Damilola Fabiyi (e-mail: samson.fabiyi@strath.ac.uk).

This work was partially supported by the Newton Research Collaboration Programme (NRCP1516/1/65) and the European Union's Horizon 2020 research and innovation programme CYBELE under grant agreement No. 825355.

ABSTRACT Inspection of rice seeds is a crucial task for plant nurseries and farmers since it ensures seed quality when growing seedlings. Conventionally, this process is performed by expert inspectors who manually screen large samples of rice seeds to identify their species and assess the cleanness of the batch. In the quest to automate the screening process through machine vision, a variety of approaches utilise appearance-based features extracted from RGB images while others utilise the spectral information acquired using Hyperspectral Imaging (HSI) systems. Most of the literature on this topic benchmarks the performance of new discrimination models using only a small number of species. Hence, it is unclear whether or not model performance variance confirms the effectiveness of proposed algorithms and features, or if it can be simply attributed to the inter-class/intra-class variations of the dataset itself. In this paper, a novel method to automatically screen and classify rice seed samples is proposed using a combination of spatial and spectral features, extracted from high resolution RGB and hyperspectral images. The proposed system is evaluated using a large dataset of 8,640 rice seeds sampled from a variety of 90 different species. The dataset is made publicly available to facilitate robust comparison and benchmarking of other existing and newly proposed techniques going forward. The proposed algorithm is evaluated on this large dataset and the experimental results show the effectiveness of the algorithm to eliminate impure species by combining spatial features extracted from high spatial resolution images and spectral features from hyperspectral data cubes.

INDEX TERMS Hyperspectral Imaging, Rice Seed Variety, Spatio-temporal Feature Fusion.

I. INTRODUCTION

Inspecting rice (Oryza sativa) seed varies is a critical procedure for quality assessment in the arable sector [1], [2], [3]. Ensuring that all seeds in a batch belong to one variety is a significant challenge for professional inspectors and farmers in seedling propagation stations. Varietal contamination can affect rice seed yields by introducing weeds and off-types into the crop while making it susceptible to disease. In turn, both factors contribute to the grade and price of produce, all of which has a high impact on large rice exporting nations such as Thailand, Vietnam and China. In a biotechnology context, where new species are engineered, the price and quality of product is affected by its originality and the certification and authorisation process is the responsibility of Rice Seed Authenticating Centres. Therefore, these centres have strict and challenging requirements to identify and confirm/authorise new rice accessions while also protecting existing rice varieties with high confidence. To fulfil such strict requirements, seedling propagation stations and plant protection centres, often utilise conventional methods that rely on extracting a sample of rice seeds from a batch and using human visual inspectors to perform manual screening. In this analysis, inspectors accept or reject grains based on their appearance by analysing features such as: shape, length, width and colour. This is a tedious, laborious, time consuming task and requires trained and experienced personnel. Automation of the inspection process would not only permit increased workforce productivity, by redeployment of personnel to more crucial tasks, but also has the potential to increase the consistency of inspections while allowing a larger number of batches/seeds to be screened with confidence.

TABLE I A SURVEY ON CURRENT PUBLICATIONS

Ref.	Number of Varieties	Extracted Features	Sensing modality	Classifier	Performance	Dataset Public	Year
Huang et al. [4]	3	Shape-based	RGB	Back-Propagation Neural Network (BPNN)	95.56%	No	2017
Hong et al. [6]	6	Morphological, colour, texture, Gist Features, Scale-Invariant Feature Transform (SIFT)	RGB	Random Forrest (RF), Support Vector Machines (SVM)	90.54%	No	2015
Lui et al. [7]	6	Colour, Morphological	RGB	Neural network	84.33%	No	2005
Peralta et al. [8]	754	Shape-based	RGB	Residual error and Average Point distance	44.8679 and 44.84528%	No	2016
Kong et al. [9]	4	Spectral	HSI	Partial Least Squares Discriminant Analysis (PLS-DA), K-Nearest Neighbor (K-NN), SVM, RF	80% - 100%	No	2013
Wang et al. [3]	3	Spectral and Morphological	HSI	Principal Component Analysis (PCA), BPNN	89.18% - 94.45%	No	2014
Vu et al. [2]	6	Spectral and Morphological	HSI	RF, SVM	84%	No	2016
Kuo et al. [11]	30	Morphological, Colour, Texture	RGB	Sparse coding	89.1%	No	2016
On Yang et al. [12]	5	Colour	RGB	BPNN	93.66%	No	2010
Aznan et al. [13]	5	Morphological	RGB	Discriminant function analysis	96%	No	2016
Pazoki et al. [14]	5	Colour, Morphological, Shape	RGB	Multi-layer perceptron, neuro-fuzzy neural networks	98.40% - 99.73%	No	2014
Sun et al. [15]	4	Spectral, texture and Morphological	HSI	SVM	91.67%	No	2015
Singh et al. [16]	4	Colour, Texture, Wavelet	RGB	BPNN	96.25 - 100%	No	2016

In the literature, a wide range of computer vision approaches have been proposed to automate the non-destructive inspection of rice seeds [4] that commonly rely on conventional RGB cameras [5], [6], [7], [8]. These approaches extract appearance-based features from the seeds such as shape descriptors, texture or colours and train models using techniques from machine learning to discriminate between species. The advent of Hyperspectral Imaging (HSI) provides an alternative sensing modality with improved discrimination performance [9] and more recent approaches combine appearance and spectral features [3], [10], [2] to increase model robustness even further.

Unlike conventional RGB imaging which measures reflectance in 3 spectral regions (Red, Green, Blue), hyperspectral imaging offers increased spectral resolution in hundreds or thousands of spectral bands. However, compared to RGB cameras, HSI hardware, typically offer reduced pixel density (~150 DPI) mainly due to spatial binning and to improve the robustness of acquired data. The reduced resolution leads to reduce fidelity in the appearance-based features especially when discriminating small objects such as rice seeds. This observation motivates the proposed approach, to build a system that combines both high spatial resolution (RGB) and high spectral resolution (HSI), sensing modalities combined with intelligent data processing techniques to perform rice seed screening automatically.

Table I lists a number of existing techniques that have been proposed in the literature in recent years. The table allows a quick comparison of existing techniques based on factors including: the number of species considered in the studies, the features extracted, the sensing modalities utilised, the algorithmic approaches taken to process the data, and, their reported performance. It can be noted that the majority of the techniques presented are applied to RGB images and almost all methods are evaluated using only a small number of different rice seed species with varying degrees of accuracy. From the review in Table I, it is not clear whether the differences in performance between existing techniques is caused by superior algorithms and the effectiveness of feature descriptors used, or, if this is simply due to differences in the inter-class or intra-class variation of species used in each study. That said, Kue et al. [11] and Peralta et al. [8] used relatively large number of species in their study having evaluated their method using 30 and 754 species and reported accuracy of up to 89.1% and 44.87% respectively. Their reported performance is not as strong as some of the other methods listed in the table, and this supports the hypothesis that other techniques do not necessarily utilise better algorithms or feature descriptors. Instead, it is possible that these techniques are evaluated in less challenging datasets with a smaller number of species which exhibit favourable intra-class and inter-class variation.

However, this hypothesis is difficult to confirm or reject as the datasets used in each paper are not publicly available.
The contributions of this paper are as follows:

1. A novel rice seed inspection system that combines a conventional RGB and hyper-spectral imaging system is proposed.
2. An innovative framework to fuse spatial and spectral data is developed and it is shown that the combined features improve discrimination ability and classification performance.
3. The performance of the proposed algorithm and system is evaluated in a large, diverse dataset of 90 rice seed varieties with 96 seeds per variety. Experiments show that varying the number of rice seeds species in the datasets can impact the classification performance and recommends that the similarity of rice seeds varieties be assessed.
4. The large dataset evaluated in this paper is made publicly available[1] to the community to assist in the benchmarking of proposed algorithms and features.

The remainder of this paper is organised as follows: Section II describes in detail, the related work. A description of the: system setup; datasets; data processing; feature extraction; classification; and species discriminant analysis technique adopted are presented in Section III. Section IV presents the experimental results and evaluates the performance of the proposed techniques on the collected dataset. Finally, Section V concludes the work and suggests future research directions.

II. RELATED WORK

Machine vision systems have been proposed for a range of food quality assessment tasks[10], [17], [18], [19]. Research has focused on combining image analysis and machine learning techniques to create new methods to perform automatic inspection and qualification. Relevant to the study presented here are rice seeds (polished) quality control or cultivar classification tasks which are specifically explored in [1]. In [1], Y. Ogawa comprehensively surveys computer vision techniques, physical property measurements, compound content and distributions of rice grains for seed quality control. Related work which specifically address non-destructive variety classification are listed in Table I.

Rice seed classification using an automatic machine-vision system usually consists of several key stages. The most important of which include image data collection, feature extraction (such as shape, size, colour, and orientation etc.) and feature representations via models using pattern recognition algorithms or multivariate analysis techniques. The appearance-based approaches often utilise morphological, colour, and textural traits, or a combination of them. As early as 1986, Lai et al. [20] proposed the use of image analysis to determine the physical dimensions of and manually classify cereal grains. Similarly, Sakai et al. [21] demonstrate the use of two-dimensional image analysis to extract dimensions and shape factors of 4 varieties of polished rice grains and manually classify them. More recent work [6], [7] and [12] focuses on rice seed variety classification tasks. Commonly, shape descriptors of the seed samples are extracted and classifiers such as Random Forests [6], Neural Networks [7] or Cubic B-Splines shape model [8] are trained.

Huang et al. [4] proposed a detailed analysis of shape descriptors that goes beyond features that are more commonly used in the literature, such as chaff tip (width, height) and depth of concavities of rice kernels. Their work shows promising results in separating visually similar species but their evaluation is limited to only 3 varieties. Kuo et al. [11] utilise multi-focus image fusion to study 30 varieties of rice seed using sparse representation classification and obtain accuracy of 89.1% with a standard derivation of 7.0%. Although, the authors briefly recognise that the majority of the literature uses a limited number of species, they do not illustrate the effect that this may have in discrimination ability. Their approach focuses on detailed Region-Of-Interest (e.g., sterile lemmas) on the grains.

Recently, HSI techniques have been used in food and agriculture engineering. Wang et al. [3] used VIS/NIR (400-1000 nm) spectral information to discriminate 3 rice varieties. The authors used a combination of: degree of chalkiness; shape features; and spectral features which are all extracted from the acquired HSI images. The dimensionality of the spectral features was reduced using Principal Component Analysis (PCA) and the resulting principal components were used to train an Artificial Neural Network, with classification accuracy of 94.45% achieved.

In [22], the authors discovered that a combination of the Least squares support vector machine (LS-SVM) regression method and VIS/NIR spectroscopy at range 325-1075 nm provides a realisable technique to monitor the nitrogen status in rice. More recently, an HSI system has been used in [9] for identifying four rice seed cultivars. By utilizing the full spectral range of their system 1,039-1,612 nm, the authors, [9], achieved results of up to 100% accuracy with a Random Forest (RF) classifier. However, four cultivars in [9] were hybridized from other species, therefore, it is unclear how the inter/intra class varies among them. Recently, work in [2] and [15] explored different feature combination schemes: spectral and texture features; morphological, texture and spectral features; and morphological and texture features while seeking the optimal feature combination. The highest accuracy in [15] was obtained when using combined spectral, morphological and texture features (91.67%, with four polished rice species). A classification accuracy of 84% was achieved in [2] utilising a combination of spectral and spatial features on a dataset of six rice seed species.

When comparing the existing techniques in the literature, one can see some shortcomings. Firstly, the performance of related techniques as listed in Table I varies significantly and there are no benchmark evaluations or common datasets to

[1] http://dx.doi.org/10.15129/b126fda2-3963-4031-ad53-e6f5fff95f8d

compare these works together. Secondly, although the results of these studies have been promising, most researchers have evaluated their methods on a relatively limited number of different rice seed species. In practical applications, an automated system faces challenges of various rice seeds. For instance, the authors in [8] also noted a very large number of rice accessions (120,000+ accessions) which are available in the TT Chang Genetic Resources Centre at the International Rice Research Institute (IRRI), Philippines. They argue that characterising shapes of the cultivated rice accessions greatly helps in authenticating new rice seeds. Kuo et al. [11] also note that rice grains of hundreds of varieties are cultivated and hence the demand for robust non-destructive authentication approaches of large number of grain seed varieties must be addressed to make solution feasible for the rice seed industry. In this study, the dataset consists of ninety rice seed varieties and is made publicly available. Both the high spatial resolution and full-band wavelengths of spectral information are fundamental resources to develop and deploy robust classifiers for performing variety classification of different rice seed species and other relevant tasks in rice seed quality inspections.

III. METHODS

A. SYSTEM SETUP

A schematic diagram of the system used for acquiring images of rice seed samples is shown in Fig. 1. It is comprised of a high resolution RGB camera and a hyperspectral imaging system. The digital camera used was a Fujifilm X-M1 with a 35mm/F2.0 lens to collect RGB images at 4,896x3,264 pixels. For gathering HSI data, a Visible - Near Infrared (VIS/NIR) range HSI system was used which consisted of a Specim V10E Imaging Spectrograph and Hamamatsu ORCA-05G CCD camera. The HSI system was configured to capture hyperspectral image data cubes in which each pixel contains a spectrum of reflected light at 256 discrete wavelengths ranging from ~ (385 – 1000) nm. Two halogen bulbs were used for illumination and these were accurately positioned to provide balanced lighting across the scene. To ensure stability, the halogen bulbs were switched on and allowed to reach constant operating temperature before the data were acquired in a dark room to minimise any other sources of illumination variance.

The Fujifilm RGB digital camera was set to operate in manual mode with an ISO of 400 and a shutter speed of 16 ms. The acquired images were saved in JPEG format and no automatic adjustment (e.g., white balance) was applied.

The HSI system is a push-broom system and hence captures HSI data in a line scan fashion. For this reason, a motorised translational stage was positioned directly beneath the imager to allow scanning. To accurately and consistently collect the data in a repeatable way, three key parameters of the HSI system needed to be adjusted and were selected as follows:

- The exposure time of the camera (e.g. 500 ms) versus the speed of movement of the translational stage (5 mm/s), which was calibrated in order to avoid spatial distortions;
- A trade-off between the exposure time and the aperture of camera (f=18) to ensure a suitable light intensity;
- The height between the lens and the stage which was set so that camera field of view captures the entire area containing all seeds in each data cube.

Prior to imaging rice seeds, images of a flat checkerboard patterns were collected for calibrating planar and lens distortion effects for the RGB and HSI sensors using the traditional camera calibration approach described in [23]. This procedure was performed once and the camera calibration parameters; i.e. rotation and transformation parameters, were stored in a XML file for aligning and registering the images acquired from both systems.

B. DATASET DESCRIPTION AND PROCESSING

Ninety known rice seed varieties were provided for this study by the National Center of Protection of New Varieties and Goods of Plants (NCPNVGGP) in Vietnam. These rice seed varieties were chosen since they are frequently planted in Vietnam to cultivate rice for consumption and exportation. The selected samples were manually screened in the traditional way by experienced technical staff at NCPNVGGP to ensure that each sample population contained only seeds which belong to the 90 species to be analysed. A single kernel from each of the 90 varieties is shown in Fig. 2.

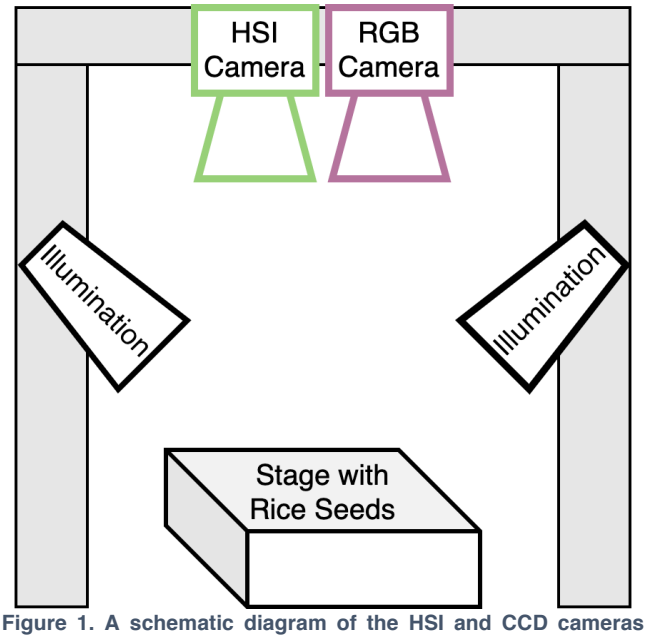

Figure 1. A schematic diagram of the HSI and CCD cameras setup for data acquisition.

For each of the 90 species considered in this work, 96 individual rice seeds were provided. The kernels from each of the 90 species were divided to 2 batches each containing 48 individual rice seed samples. Each set of 48 seeds was then positioned on a white sheet of paper in a (6 x 8) matrix structure and imaged using the HSI system and the digital RGB camera. Thus, each of the 90 species of rice seeds were captured in 2 hyperspectral data cubes and 2 high resolution RGB images each containing 48 different seeds. In total, the

dataset consists of fully registered RGB and HSI images ~ (385 – 1000) nm of 8640 seeds (90 varieties x 96 seeds). In this study the seeds were manually positioned on the white sheet to avoid overlaps or touching boundaries between them. In practice, one can conceive a conveyor belt arrangement where seeds are mechanically spread individually under appropriate and consistent illumination for imaging

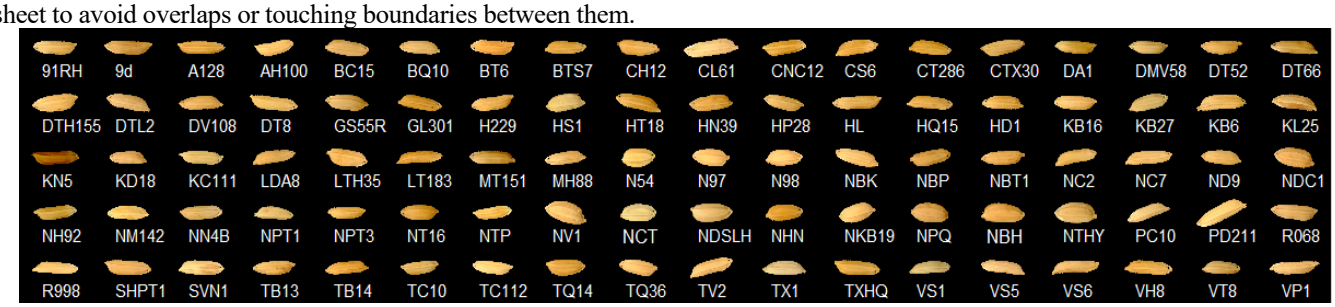

Figure 2. Photos of rice seed samples of 90 species. The short name of each species is given beneath each kernel

The data processing steps to extract spatial and spectral features is illustrated in Fig. 3. Initially, both image modalities are calibrated for lens and planar effects using the rotation and transformation matrix obtained from the checkerboard pattern as described in Section III-A. Then, the HSI data cube is normalised as described in Section III-D. After this, the processing paths diverge slightly. The RGB data are segmented using the process described in Section III-C and binary masks for each rice seed in the RGB image are used to extract the high resolution spatial features as described in Section III-D.

The masks obtained from the RGB segmentation are then transformed to the HSI space (using the calibration matrix obtained from imaging the checkboard pattern) to segment the rice seeds in the HSI data. The segmented seeds are subsequently used to extract the spectral features as described in Section III-E.

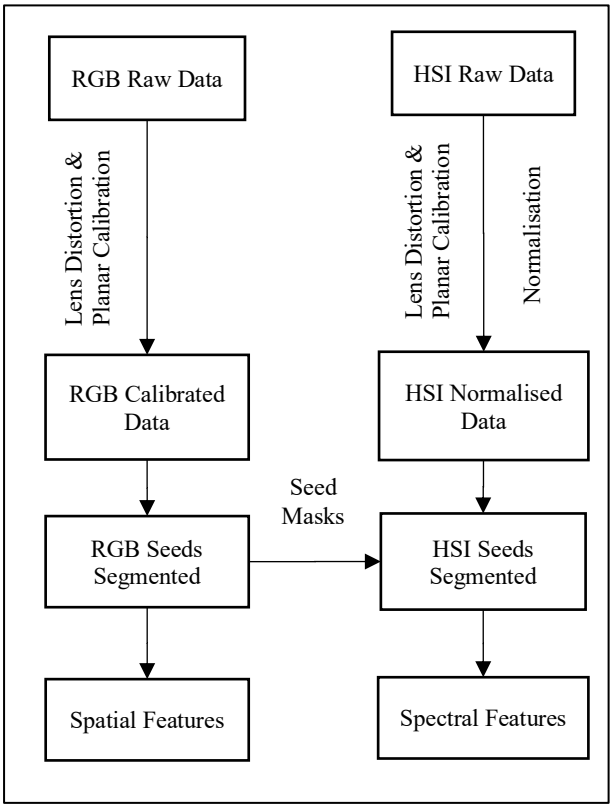

Figure 3. A block diagram showing the stages of the data processing task.

Figure 4. Results of the spatial feature extraction. The ID number of each seed is shown to its right. For illustration purposes, only features f4 and f6 are shown below each kernel. The MajorAxisLength f2 and MinorAxisLength f3 are marked with a red and a blue line, respectively.

C. CALIBRATION PROCEDURES AND RICE SEED SEGMENTATION

The rice seed segmentation is performed on the high spatial resolution RGB images to ensure that the complete kernel is captured. The proposed procedure consists of the following steps. First, the R-channel of the RGB image is extracted; the R-Channel is chosen because it offers the highest contrast to the background. A top-hat transform [24] of the R-channel is then computed and thresholded to obtain the binary images.

D. SPATIAL FEATURE EXTRACTION

Trained personnel screen rice seeds by manually analysing their spatial features. In this work, spatial features of the

separated seeds are extracted from RGB image masks to encapsulate the expert knowledge. The features extracted are selected due to their effectiveness for discriminating among species, as shown in recent work, [6] and [7]. The morphological feature vector *f* for a single kernel contains the following six attributes:

f_1: Area; the number of pixels inside a seed kernel

f_2, f_3: Major Axis Length and Minor Axis Length; specify the length (in pixels) of the major and minor axis of the ellipse that has the same normalised second central moment at the region of the sample seed

f_4: Aspect Ratio; the ratio of Minor Axis Length over the Major Axis length ($\frac{f_3}{f_2}$)

f_5: Perimeter over Area Ratio; $\frac{Perimter}{Area}$, where Perimeter is number of pixels along the seed boundary;
and Area is the f_1 feature.

f_6: Eccentricity; FociDistance/MajorAxisLength (i.e. the eccentricity of the ellipse with the same second moments as the seed kernel region) is the distance between two foci of the ellipse, and the major axis length of the ellipse (i.e. feature)

illustrated in Fig. 3. Firstly, to reduce the variation in the acquired reflectance values among measurements, the collected data are corrected following the approach laid out in [25]. Let *y* denote a data cube consisting of reflectance values as a two-parameter set:

$$y_\lambda(x), x \in X, \lambda \in \Lambda \qquad (1)$$

where λ represents a wavelength belonging to Λ, that is a set of the wavelengths at VIS/NIR range ~ (385 – 1000) nm and *x* represents a pixel in *X* where *X* is 2-D coordinate by row *m* and column *n*. For each specific wavelength, the array of reflectance values can be regarded as an image where spatial relationships between the pixel reflectance values have meanings. At each *x*, the raw reflectance value could vary due to different lighting conditions. To reduce the variation in the acquired reflectance values due to illumination variations or unique pixel response, the data were scaled relative to known max reflectance value; the raw data are normalised using:

$$y_\lambda(x) := \frac{y_{raw,\lambda}(x) - b(n,\lambda)}{w(n,\lambda) - b(n,\lambda)}, \lambda \in \Lambda \qquad (2)$$

where $b(n,\lambda)$ and $w(n,\lambda)$ are the reflectance values of reference

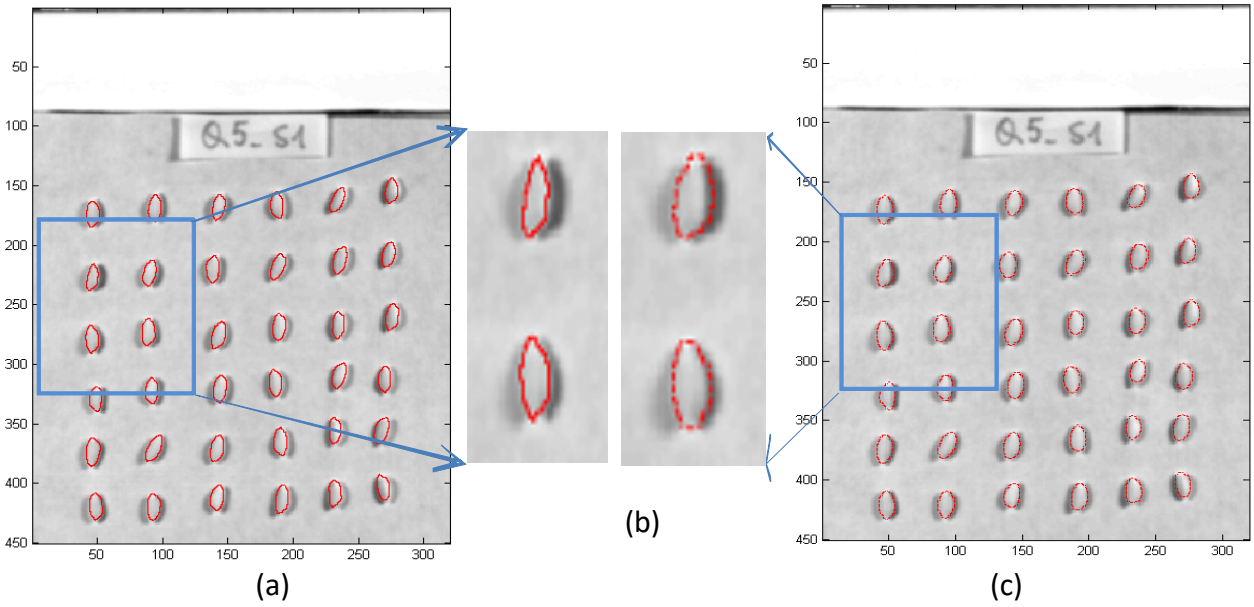

Figure 5. Comparing segmentation results of rice seeds on HSI image. (a) Using RGB image for reference (b) A Zoom-in version of two segmentation results (Red and white points are the results from (a) and (c) respectively) (c) Without using RGB image.

Fig. 4 illustrates output of the spatial feature extraction for a sample image that contains 48 seeds. It is noted that because the spatial features are extracted using the high spatial resolution images, they are expected to be more accurate than those reported in [2], [15] where the spatial features are extracted from the HSI system which has lower spatial resolution.

E. SPECTRAL FEATURE EXTRACTION

Extracting the spectral information consists of two main phases: data correction, and feature extraction. These are

dark and white images. The dark reference is acquired by covering the lens-cap and the white reference is a 100% reflective spectralon tile which is a highly reflective Lambertian scatter commonly used to calibrate HSI systems. For each λ, $b(n)$ and $w(n)$ are averaged on reflectance values at column *n* along the white tile's height dimension. After normalizing the spectral data, the rice seed masks obtained from the above description of the rice seeds segmentation procedure are transformed to the HSI plane using a transformation matrix including rotation and translation operators to segment the seed samples on the spectral images,

as shown in Fig. 3. Fig. 5 clearly illustrates the advantages of the proposed segmentation method compared to the conventional work (e.g., in [2], [15]) where the seed segments are extracted directly from the low spatial resolution images collected by HSI system. When the seeds are segmented using only the HSI data, in many cases, the segments include some pixels at boundary regions of the shadow rather than the pure spectra of the seeds themselves. Subsequently, any measurements of the morphological features made using only spectral image segmentation could become inaccurate and spectra of non-rice-seed pixels will be included in the analysis. Hence, in this work the seeds are segmented from the high resolution RGB image to ensure that the spatial and spectral features are correctly included in the analysis.

Based on the segmented seed samples on a hyperspectral data cube, spectral information from every pixel of the seed regions is extracted. The mean spectrum of all pixels in each seed is then computed and used to determine the spectral features for that seed. As denoted in (2), a raw spectral feature vector of a rice seed sample is a set of y_λ in which λ is one of the 256 bands belonging to a range $\Lambda \sim (385 - 1000)$ nm for our VIS/NIR system.

F. DIMENSIONALITY REDUCTION

Originally collected spectra are high dimensional feature sets. LDA is a statistical tool that can be used to reduce the dimensionality of data [26]. For this application, LDA is used to select features that account for the highest degree of variation among the 90 species in the dataset and select variables for classification or discriminant analysis of the rice seed species. In LDA, features are ranked based on the amount of variation they account for in the data. LDA is a supervised algorithm and so uses the labels provided in the dataset. In this work, LDA was adopted because it maximizes the separability of the different rice seed species. LDA can be used to reduce the dimensionality of the spectral features (originally 256) in the dataset by maximizing the separation among the 90 species of rice seeds. The transform achieves this by maximizing the distance between the means of 90 species (interclass variance) and minimizing the variation within each category (intra-class variance) itself [27]. In section IV, the spatial features are combined with varying number of LDA features to determine the best feature combination scheme for performing rice seed classification using our dataset.

G. RICE SEED VARIETY CLASSIFIER

The aim of variety classification is to detect seeds within a batch which are not of the species that the batch is claimed to represent. Models which are trained to perform this task could directly utilize the full-band wavelengths or only selected components (for spectral features) from the output of feature extraction or dimensionality reduction techniques adopted, and/or spatial context. Therefore, the features extracted are utilized in four different schemes: (1) spatial features only, (2) spectral features only, (3) a combination of all 256 spectral features and extracted spatial features; (4) a combination of LDA components extracted from the spectral data fused with the spatial features. For the task of rice seed variety classification, a Random Forest (RF), which has produced better classification results than many other classifiers including support vector machines and K-Nearest Neighbor in many related work [6], [9], [2], is trained for rice seed classification.

Random forests contain many decision trees which are grown from a bootstrap sample of the response variable. Trees are allowed to grow to a maximum extent without pruning after selection of the best split from a random subset of features at each of the decision trees' nodes. Accumulating the results of each decision tree forms the basis on which random forests make predictions on new data. Random forests are able to process large datasets in a fast, effective way while achieving high classification accuracy. The number of decision trees and the ratio of the training to test samples that gave the best classification results during preliminary analysis are 500 and 4:1 respectively, and so are adopted for this work.

IV. EXPERIMENTAL RESULTS AND ANALYSIS

In order to evaluate the performance of our RF classifier and the effectiveness of the approaches proposed in this work, three performance metrics are used. They are Precision, P, Recall, R, and F_1 Score.

$$P = \frac{t_p}{t_p + f_p} \qquad (3)$$

$$R = \frac{t_p}{t_p + f_n} \qquad (4)$$

where t_p is the number of true positives, f_p is the number of false positives, t_n is the number of true negatives and f_n is the number of false negatives. The F_1 score is the harmonic mean of the precision and recall,

$$F_1 \text{ score} = 2 * \frac{P*R}{P+R} \qquad (5)$$

Based on the collected datasets of ninety species, and in line with the objectives of this work, results and analysis are presented in this section under three different scenarios. The first and second scenarios aim to show the effectiveness of using spatial and spectral features extracted from a high resolution RGB image fused with HSI data for rice seed classification. In the first scenario, the RF classifier was trained using all 90 species. Since we are also interested in exploring how the number of species in the dataset affects classifier performance, we considered a second scenario where 6 different subsets of the datasets were used to train the classifier separately and evaluate performance. Each of the 6 subsets of the data consists of 6 species (more than or similar to the typical number used in related work – see Section I, Table I) drawn randomly from the 90 available. In the third scenario, we select a different 6 subsets of the data and vary the number of species in each subset from 6 – 90 to explore how increasing the number of species in the dataset affects classifier performance. For each sub-dataset, the performance of the random forest is reported and analysed.

A. ANALYSING PERFORMANCE ON ALL 90 SPECIES

In this experiment, we trained 4 different RF models using different combinations of the data we gathered for training and testing. The classification results presented in Table II, illustrate that the average precision, average recall and average F_1 score were lowest when using only spatial features to train our RF. The average precision, average recall and average F_1 score improved when only spectral features were used. As expected, higher average precision, average recall and average F_1 scores were achieved when the spatial and spectral features were combined and analysed together. Next, we used LDA to reduce the dimensionality of the spectral features (originally 256) in the dataset. The outputs of the LDA were separately combined with the spatial features extracted from our dataset of 90 species. These data were used to train the RF classifier. The classification results obtained when using this approach to differentiate between all 90 species are presented in Table II and Fig. 6. By applying the dimensionality reduction technique, the performance of the RF classifier was significantly improved when compared to our earlier analyses thus validating the usefulness of our approach. From Fig. 6, we observed that the spatial features and 85 LDA components provides the best classification results with average precision, average recall and average F_1 score of 79.64%, 78.80% and 78.27% respectively for all 90 species. While we have discussed the average precision, recall and F_1 score here, we also show the individual scores for each of the 90 species in Table III. Interestingly, the F_1 scores vary between 80-100%, and 90-100% for 45 and 22 varieties respectively. These results showed very high F_1 scores and are comparable with those reported in Table I. These results are pointers to the potential of our new imaging modality (combining spatial features from RGB images and spectral features from hyperspectral images) for rice seed discrimination even with a fairly large number of species. However, we also note that this technique, when used on the entire dataset of 90 species, performs better for some species than others as illustrated in Table III. Further analysis carried out to find out what could be responsible for this is presented in section IV-C.

TABLE II CLASSIFICATION RESULTS WITH AND WITHOUT DIMENSIONALITY REDUCTION

Feature Schemes	Average precision (%)	Average Recall (%)	Average F1 Score (%)
spatial	16.33	16.57	15.96
spectral	34.93	35.86	34.46
Spatial + spectral on full bands	51.66	51.49	50.51
Spatial + 85 LDA Components from Spectral	79.64	78.80	78.27

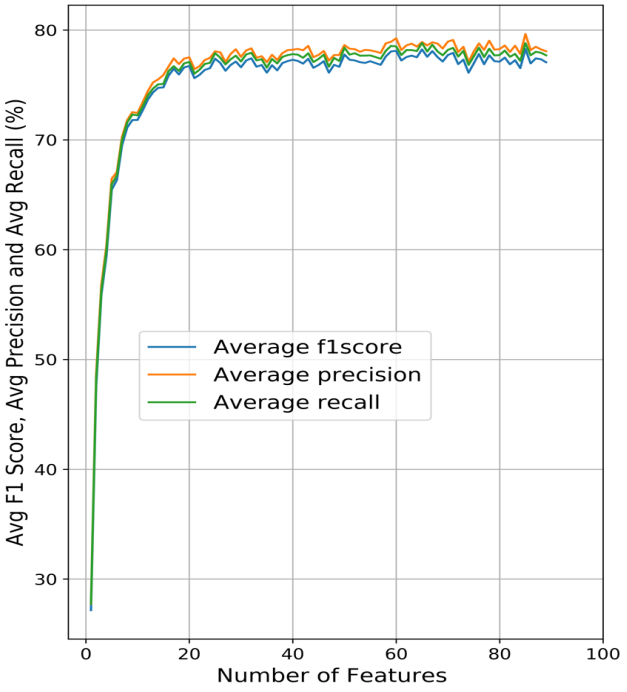

Figure 6. Classification result using the outputs of LDA and 90 species

B. ANALYSING SELECTED SUBSETS OF 6 SPECIES

In this scenario, we selected 6 subsets from our dataset in order to compare our algorithm with state-of-the-art techniques which (as shown in Table I) tend to be evaluated on a small variety of species; typically, 5-6 with the exception of [11] (30 species) and [8] (754 species). 5 of the 6 subsets selected, each consisted of 6 randomly selected species while the 6th subset consists of species that exhibited the worst discrimination performance in Table III. All the subsets are summarized in Table IV. We used LDA to extract features from the spectral data of each subset and combined the outputs with corresponding spatial features using the best feature combination scheme selected. The 6 subsets were used separately to train the RF classifier and the classification results are presented in Table V. We also note that the computation time (segmentation and classification) is 0.53 s on a commodity hardware; Intel Core i7. The computation time is insignificant for practical application of screening rice seeds compared to a manual human screening which takes minutes. For the first 5 subsets studied, we observed that the average precision and average recall were significantly improved when compared to the performance of the 90 species classification results. Our novel approach produced very high average F_1 scores and outperformed equivalent scores reported for the state-of-the-art techniques listed in Table I except for those in [9], [14] and [16]. This experiment shows that, in line with state-of-the-art techniques for rice seed classification, very good results and elimination of impure species from rice seed samples can be achieved by taking

TABLE III CLASSIFICATION RESULTS WITH THE BEST FEATURE SCHEME, SPATIAL + 85 LDA FEATURES, AND 90 SPECIES

Labels	Precision	Recall	F1 score	Labels	Precision	Recall	F1 score	Labels	Precision	Recall	F1 score
GS55R	100.00	100.00	100.00	LTH35	89.47	80.95	85.00	KN5	62.50	90.91	74.07
TC10	100.00	100.00	100.00	PD211	82.61	86.36	84.44	TV2	78.57	68.75	73.33
NV1	100.00	100.00	100.00	LT183	75.00	95.45	84.00	DTH155	81.25	65.00	72.22
KL25	100.00	100.00	100.00	PC10	81.82	85.71	83.72	ND9	68.18	75.00	71.43
N97	100.00	100.00	100.00	HQ15	73.91	94.44	82.93	KB6	73.33	68.75	70.97
NPQ	96.00	100.00	97.96	KD18	87.50	77.78	82.35	NBH	77.27	65.38	70.83
NT16	95.24	100.00	97.56	TB14	94.12	72.73	82.05	GL301	60.87	82.35	70.00
BT6	100.00	94.74	97.30	NTP	72.73	94.12	82.05	NH92	66.67	71.43	68.97
HS1	100.00	94.12	96.97	NTHY	76.47	86.67	81.25	DMV58	66.67	71.43	68.97
TXHQ	93.75	100.00	96.77	NDSLH	76.47	86.67	81.25	NBP	75.00	62.50	68.18
NCT	100.00	92.86	96.30	VS6	78.95	83.33	81.08	NM142	66.67	66.67	66.67
N54	92.31	100.00	96.00	DA1	80.00	80.00	80.00	LDA8	55.17	84.21	66.67
CS6	93.33	93.33	93.33	NC7	87.50	73.68	80.00	NC2	54.17	81.25	65.00
NPT3	93.33	93.33	93.33	MH88	73.68	87.50	80.00	HD1	60.00	70.59	64.86
CL61	89.47	94.44	91.89	NN4B	79.17	79.17	79.17	VP1	66.67	62.50	64.52
DT66	85.00	100.00	91.89	AH100	70.83	89.47	79.07	VS1	51.61	84.21	64.00
VT8	100.00	84.21	91.43	SVN1	81.82	75.00	78.26	DT8	57.89	68.75	62.86
SHPT1	95.45	87.50	91.30	A128	84.21	72.73	78.05	H229	69.23	56.25	62.07
VH8	95.24	86.96	90.91	CT286	80.00	76.19	78.05	TX1	100.00	44.44	61.54
N98	95.00	86.36	90.48	CH12	76.19	80.00	78.05	HP28	71.43	52.63	60.61
NHN	95.00	86.36	90.48	TQ14	72.73	84.21	78.05	MT151	100.00	42.86	60.00
R068	91.67	88.00	89.80	KB27	73.68	82.35	77.78	BC15	56.25	64.29	60.00
NDC1	95.45	84.00	89.36	91RH	100.00	62.50	76.92	CNC12	100.00	42.11	59.26
BQ10	95.45	84.00	89.36	CTX30	83.33	71.43	76.92	KC111	72.73	50.00	59.26
DTL2	87.50	91.30	89.36	R998	66.67	90.00	76.60	NBK	69.23	47.37	56.25
HN39	84.21	94.12	88.89	HT18	81.25	72.22	76.47	DT52	64.29	50.00	56.25
HL	85.71	90.00	87.80	TC112	81.25	72.22	76.47	NBT1	50.00	50.00	50.00
DV108	80.00	94.12	86.49	BTS7	66.67	88.89	76.19	NPT1	40.00	40.00	40.00
9d	86.36	86.36	86.36	TQ36	64.00	94.12	76.19	TB13	42.86	35.29	38.71
NKB19	82.14	88.46	85.19	VS5	76.19	76.19	76.19	KB16	33.33	30.77	32.00

advantage of spatial features from high spatial resolution images and combining them with spectral features from hyperspectral data cube. For the last subset of species, the average F1 score when employing the first classifier trained on 90 varieties is 45.54%. In contrast, when the RF classifier is trained specifically on the 6 species selected, the F1 score rises to 61.29%. This improvement comes as a result of the smaller dataset and suggests that when the species are known a-priori, a targeted classifier would be more appropriate.

C. ANALYSING THE SUBSETS WITH VARYING SPECIES SIZES

From the results presented in Sections B and C, it is clear that the size of the dataset and variety of species considered in each experiment directly affects our RF classifier's performance. To explore this further, we selected a further 6 subsets of data from our set of 90 species. This time, we varied the number of species in each subset of data to include 6, 20, 40, 60, 80 and 90 different species to allow us explore exactly how varying number of species in a study can influence our classifier's performance. Having prepared the data, we applied LDA to extract features from the spectral data of each of our data subsets of increasing size and we combined the outputs with corresponding spatial features. We then trained the RF classifier using the output of LDA (starting from 1 LDA component up to S-1, where S is the number of species in the dataset) combined with spatial features in order to determine the number of features that gives the best performance. For each subset of the data considered, we obtained a plot of average F1 score against the number of LDA features used in the classification. The results of this are shown in Fig. 7. We also obtained the maximum average F1 score from each of the plots in Fig. 7 and used this information to plot the maximum average F1 score as a function of the number of species considered as shown in Fig. 8. From Fig. 8, we observed that the performance of the RF classifier appears to be impacted by the number of species used in the study. The average F1 scores significantly dropped from 98.17% for 6 species to 78.27% for 90 species. One reason for this drop in classifier performance could be due to an increase in the level of similarity among the rice seeds species as the number of varieties also increases.

TABLE IV SPECIES CONTAINED IN EACH SUB-DATASET

Subset	Species
1	HS1, CH12, AH100, SVN1, 91RH, DT8
2	TB14, N54, NKB19, HQ15, BT6, NC7
3	KB6, AH100, HQ15, TQ14, KL25, NHN
4	TC10, DTL2, KB16, BT6, KB27, CNC12
5	CL61, NKB19, VH8, TX1, MT15, HL
6	NBK, DT52, NBT1, NPT1, TB13, KB16

TABLE V CLASSIFICATION RESULTS USING THE OUTPUT OF LDA AND RANDOMLY DRAWN 6 SPECIES

Subsets	Average precision (%)	Average Recall (%)	Average F1 Score (%)	Min–Max F1 score (%)
1	96.03	96.46	96.18	89.66-100
2	96.23	96.31	96.21	89.47-100
3	98.59	98.33	98.42	97.30-100
4	98.55	97.93	98.17	95.45-100
5	96.39	96.73	96.52	92.86-100
6	61.99	61.12	61.29	35.71 - 85.71

As a result, the need to investigate the influence of similarities among species of rice seeds on the classifiers' performance becomes imperative. Furthermore, we reported in the previous subsection that the approaches utilized in [9], [14], and [16] attained better results than ours. Similarity assessment of rice seeds species will also help to clarify whether the higher performances reported in these papers is due to the use of better feature combination schemes, better algorithms or inter/intra class variation among species themselves. While in general the algorithm presented in this papers performs very well, our technique does have some limitations. This is clear by analysing situations where the method does not perform well. For example, some of the species which have poor classification such as species TB13, KB16, NBK and NPT1 all have virtually identical spectral profiles. This is clear with reference to Figures 9 - 12 and results in the misclassification of some seeds by the proposed method. Future work will be focused on the proposition of techniques to assess how similar these species of rice seeds are and to mitigate degrading effects on the classifiers' performance due to the level of similarities. While it is believed that misclassifications occur due to species exhibiting similar properties, it should be noted that that the observed drop in performance could also be due to the limited number of rice seeds/kernels available versus what is required to cover the large feature space. Going forward, the effects of varying and, in particular, increasing the number of rice seeds per class will be explored.

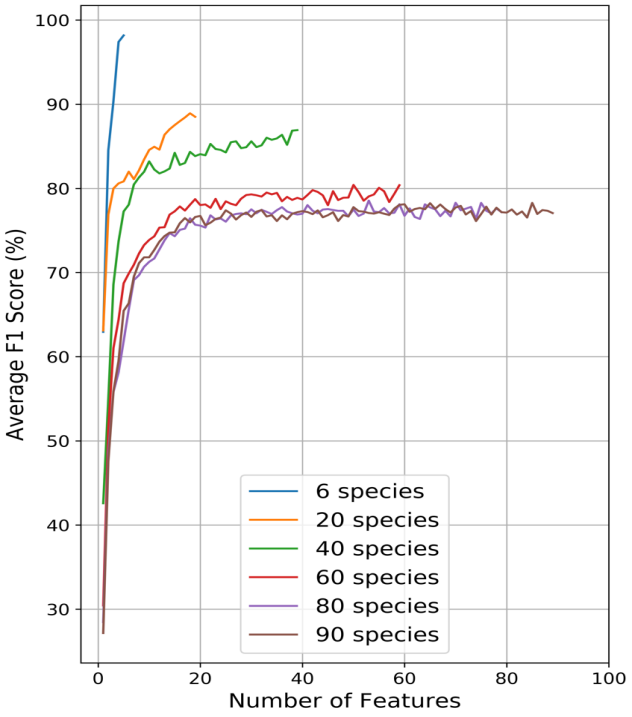

Figure 7. Plots of average F_1 scores against number of features for sub-datasets with species sizes of 6, 20, 40, 80, and 90

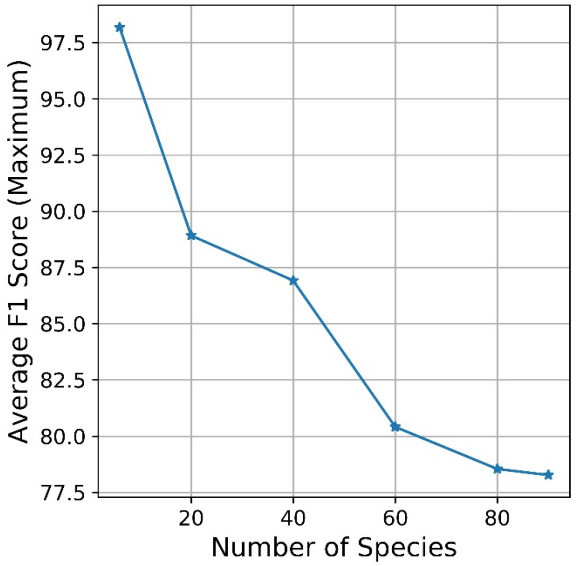

Figure 8. A plot of maximum average F_1 score against number of species

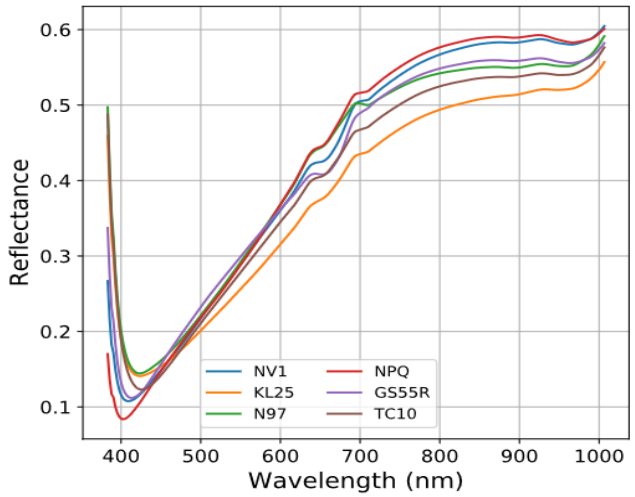

Figure 9. Average spectral profiles of some species with good classification results in Table III

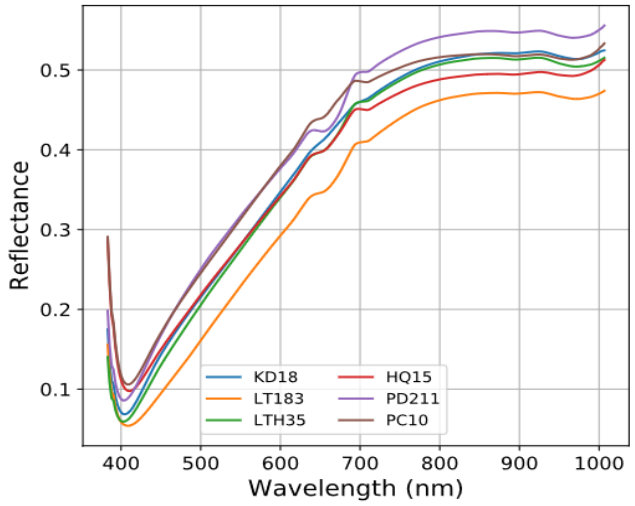

Figure 10. Average spectral profiles of some species with good classification results in Table III

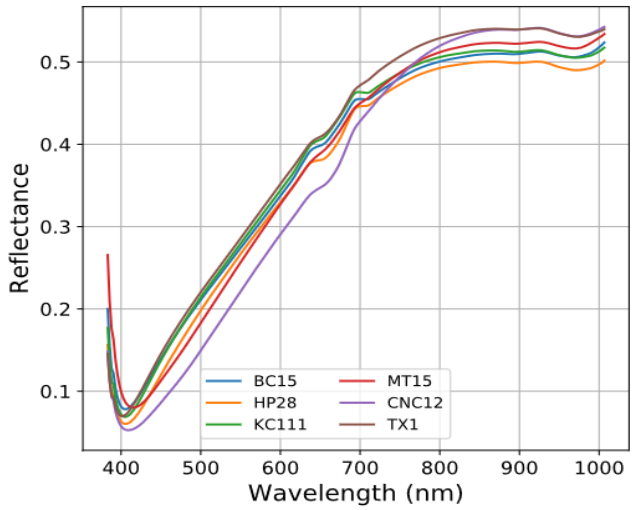

Figure 11. Average spectral profiles of some species with poor classification results in Table III

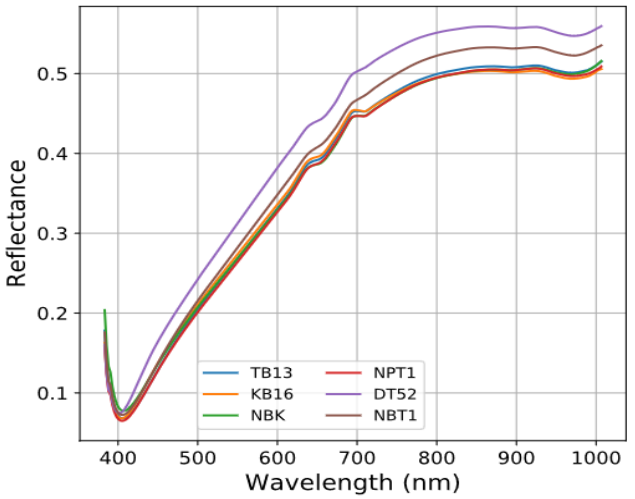

Figure 12. Average spectral profiles of some species with poor classification results in Table III

V. CONCLUSION

This paper presents a new RGB and HSI system for rice seed variety classification. RGB images and hyperspectral image data cubes which offer high spatial and spectral resolution respectively were acquired using the proposed system. A large number of rice seed species (90 specifically) were selected and the spatial and spectral features extracted from the acquired images and data cube constitute the dataset which was used for this work and is made publicly available. Experimental results show that very good classification results and elimination of impure species from rice seed samples can be achieved by taking advantage of spatial features from high spatial resolution images and fusing them with spectral features from hyperspectral data cubes. Suboptimal performance reported for some categories was linked to the use of samples with large number of species and similarities among species. Future work will focus on assessing the similarities among species of rice seeds and exploring ways in which the degrading effects on classifiers' performance due to seed similarty can be mitigated. We will also aim to explore how increasing the number of seeds per class during training can improve the results. Finally, we intend to evaluate the performance of the proposed techniques using an NIR spectral data (1000-1700nm). In this work, our novel approach was applied on a large set of 90 rice seeds provided by the National Center of Protection of New Varieties and Goods of Plants (NCPNVGGP) in Vietnam. This approach can be extended to datasets with larger number of species which are available at other agricultural institutes.

ACKNOWLEDGMENT

The authors are thankful to the Newton Research Collaboration Programme (NRCP1516/1/65) for the financial support and the National Centre of Protection of New Varieties and Goods of Plants (NCPNVGGP) in Vietnam for providing the rice seeds for this work. The project was

partially funded from the European Union's Horizon 2020 research and innovation programme CYBELE under grant agreement No. 825355.

REFERENCES

[1] Y. Ogawa, "Quality Evaluation of Rice," Comput. Vis. Technol. Food Qual. Eval., pp. 377–400, Jan. 2008.

[2] H. Vu et al., "Spatial and spectral features utilization on a Hyperspectral imaging system for rice seed varietal purity inspection," in 2016 IEEE RIVF International Conference on Computing & Communication Technologies, Research, Innovation, and Vision for the Future (RIVF), 2016, pp. 169–174.

[3] L. Wang, D. Liu, H. Pu, D. W. Sun, W. Gao, and Z. Xiong, "Use of Hyperspectral Imaging to Discriminate the Variety and Quality of Rice," Food Anal. Methods, vol. 8, no. 2, pp. 515–523, 2015.

[4] K. Y. Huang and M. C. Chien, "A novel method of identifying paddy seed varieties," Sensors (Switzerland), vol. 17, no. 4, pp. 1–8, Apr. 2017.

[5] CHENG Fang, LIU Zhao-yan, and YING Yi-bin, "Machine Vision Analysis of Characteristics and Image Information Base Construction for Hybrid Rice Seed," Rice Sci., vol. 12, no. 1, pp. 13–18, 2005.

[6] P. T. T. Hong, T. T. T. Hai, L. T. Lan, V. T. Hoang, V. Hai, and T. T. Nguyen, "Comparative Study on Vision Based Rice Seed Varieties Identification," in Proceedings - 2015 IEEE International Conference on Knowledge and Systems Engineering, KSE 2015, 2016, pp. 377–382.

[7] Z. Liu, F. Cheng, Y. Ying, and X. Rao, "Identification of rice seed varieties using neural network," J. Zhejiang Univ. Sci., vol. 6B, no. 11, pp. 1095–1100, Oct. 2005.

[8] C. N. M. Peralta, J. P. Pabico, and V. Y. Mariano, "Modeling shapes using uniform cubic B-splines for rice seed image analysis," in 2016 IEEE 6th International Conference on Communications and Electronics, IEEE ICCE 2016, 2016, pp. 326–331.

[9] W. Kong, C. Zhang, F. Liu, P. Nie, and Y. He, "Rice seed cultivar identification using near-infrared hyperspectral imaging and multivariate data analysis," Sensors (Basel)., vol. 13, no. 7, pp. 8916–8927, 2013.

[10] D.-W. Sun, Computer vision technology for food quality evaluation. Elsevier/Academic Press, 2008.

[11] T. Y. Kuo, C. L. Chung, S. Y. Chen, H. A. Lin, and Y. F. Kuo, "Identifying rice grains using image analysis and sparse-representation-based classification," Comput. Electron. Agric., vol. 127, no. 9, pp. 716–725, Sep. 2016.

[12] A. G. OuYang, R. J. Gao, Y. De Liu, X. D. Sun, Y. Y. Pan, and X. L. Dong, "An automatic method for identifying different variety of rice seeds using machine vision technology," in Proceedings - 2010 6th International Conference on Natural Computation, ICNC 2010, 2010, vol. 1, pp. 84–88.

[13] A. A. Aznan, I. H. Rukunudin, A. Y. M. Shakaff, R. Ruslan, A. Zakaria, and F. S. A. Saad, "The use of machine vision technique to classify cultivated rice seed variety and weedy rice seed variants for the seed industry," Int. Food Res. J., vol. 23, pp. S31 – S35, 2016.

[14] A. R. Pazoki, F. Farokhi, and Z. Pazoki, "Classification of rice grain varieties using two artificial neural networks (mlp and neuro-fuzzy)," J. Anim. Plant Sci., vol. 24, no. 1, pp. 336–343, 2014.

[15] J. Sun, X. Lu, H. Mao, X. Jin, and X. Wu, "A Method for Rapid Identification of Rice Origin by Hyperspectral Imaging Technology," J. Food Process Eng., vol. 40, no. 1, p. e12297, Feb. 2017.

[16] K. R. Singh and S. Chaudhury, "Efficient technique for rice grain classification using back-propagation neural network and wavelet decomposition," IET Comput. Vis., vol. 10, no. 8, pp. 780–787, May 2016.

[17] A. Polak, F. K. Coutts, P. Murray, and S. Marshall, "Use of hyperspectral imaging for cake moisture and hardness prediction," IET Image Process., vol. 13, no. 7, pp. 1152–1160, May 2019.

[18] T. Qiao, J. Ren, C. Craigie, J. Zabalza, C. Maltin, and S. Marshall, "Quantitative Prediction of Beef Quality Using Visible and NIR Spectroscopy with Large Data Samples Under Industry Conditions," J. Appl. Spectrosc., vol. 82, no. 1, pp. 137–144, Mar. 2015.

[19] T. Kelman, J. Ren, and S. Marshall, "Effective classification of Chinese tea samples in hyperspectral imaging," Artif. Intell. Res., vol. 2, no. 4, 2013.

[20] F. S. Lai, I. Zayas, and Y. Pomeranz, "Application of pattern recognition techniques in the analysis of cereal grains," Cereal Chem., vol. 63, no. 2, pp. 168–172, 1986.

[21] N. Sakai, S. Yonekawa, A. Matsuzaki, and H. Morishima, "Two-dimensional image analysis of the shape of rice and its application to separating varieties," J. Food Eng., vol. 27, no. 4, pp. 397–407, Jan. 1996.

[22] Y. Shao, C. Zhao, Y. Bao, and Y. He, "Quantification of Nitrogen Status in Rice by Least Squares Support Vector Machines and Reflectance Spectroscopy," Food Bioprocess Technol., vol. 5, no. 1, pp. 100–107, Jan. 2012.

[23] Z. Zhang, "A Flexible New Technique for Camera Calibration," 2000.

[24] X. Bai, F. Zhou, and Y. Xie, "New class of top-hat transformation to enhance infrared small targets," J. Electron. Imaging, vol. 17, no. 3, p. 030501, Jul. 2008.

[25] P. Geladi, J. Burger, and T. Lestander, "Hyperspectral imaging: calibration problems and solutions," vol. 72, no. 2, pp. 209–217, 2004.

[26] W. Li, F. Feng, H. Li, and Q. Du, "Discriminant Analysis-Based Dimension Reduction for Hyperspectral Image Classification: A Survey of the Most Recent Advances and an Experimental Comparison of Different Techniques," IEEE Geosci. Remote Sens. Mag., vol. 6, no. 1, pp. 15–34, Mar. 2018.

[27] A. Tharwat, T. Gaber, A. Ibrahim, and A. E. Hassanien, "Linear discriminant analysis: A detailed tutorial," vol. 30, no. 2, pp. 169–190, 2017.

[28] A. Zimek, E. Schubert, and H.-P. Kriegel, "A survey on unsupervised outlier detection in high-dimensional numerical data," Stat. Anal. Data Min., vol. 5, no. 5, pp. 363–387, Oct. 2012.

[29] R. J. Durrant and A. Kabán, "When is 'nearest neighbour' meaningful: A converse theorem and implications," J. Complex., vol. 25, no. 4, pp. 385–397, Aug. 2009.